ISSN (Print) 1226-1750
ISSN (Online) 2233-6656
Journal of Magnetics 31(1), 35-38 (2026) https://doi.org/10.4283/JMAG.2026.31.1.35

Magnetic and Hyperthermia Properties of $Co_xFe_{3-x}O_4$ (x=0.2, 0.4, 0.6, 0.8, 1.0)

J.-H. Kang and Sam Jin Kim*

Department of Physics, Kookmin University, Seoul 02707, Republic of Korea

(Received 12 January 2026, Received in final form 24 February 2026, Accepted 24 February 2026)

Nanoparticle samples $Co_xFe_{3-x}O_4$ (x=0.2, 0.4, 0.6, 0.8, 1.0) are manufactured using high temperature thermal decomposition (HTTD) method. Each sample is confirmed to have a single structural phase with a group of Fd-3m spaces by Rietveld refinement of the XRD diffraction spectra. The lattice constant increases linearly from 8.3759 Å for x=0.2, to 8.3965 Å for x=1.0. Through the VSM experiment, magnetic properties are verified by measuring magnetization and coercive force up to 15 kOe at room temperature. For x=0.8 samples, the saturation magnetization and coercive force field are M_s=71.9 emu/g and H_c=40.5 Oe, respectively. The hyperthermia test results show that the self-heating temperature of the sample x=0.8 was 63.7 °C under an alternating magnetic field of 250 Oe at 112 kHz. Successful superparamagnetic nanoparticles with doping fabrication can achieve high magnetization but low coercivity, which is suitable for hyperthermia.

Keywords : hyperthermia, nanoparticles, superparamagnetic materials, co doped ferrite, spinel structure

1. Introduction

Recently, there has been extensive research on nano-ferrites, which are regarded as a hyperthermia material [1-5]. Magnetic hyperthermia materials have been developed with a view to cancer treatment. Under varying magnetic field, it gives strong heat but quite selective thermal radiation attack to cancer cells. Many researchers are studying various forms of spinel ferrite being composed of two crystalline sublattices, tetrahedral (A) and octahedral (B) site, described as AB_2O_4 [6]. Spinel material is advantageous because of wide range doping possibility and synthetic accessibility. Attempts to utilize the properties of exothermic reaction and soft-ferrites characterization by substituting the transition element (Fe^{2+}, Cu^{2+}, Zn^{2+}, Ni^{2+}, Co^{2+}, etc.), on B-sites have been actively studied [7, 8]. For examples, a group of authors reported on Mössbauer studies and hyperthermia properties for Gd substituted Fe_3O_4 [9, 10].

In this study, we examined the hyperthermia properties of Co ion substituted $Co_xFe_{3-x}O_4$ (x=0.2, 0.4, 0.6, 0.8, 1.0), which combines a typical soft-ferrite material, Fe_3O_4, with a typical hard magnetic one $CoFe_2O_4$, having a greater coercive field. The replacement of Co^{2+} can cause changes in coercivity due to the contribution of none-zero orbital angular momentum of Co^{2+} ions. Substituting Co^{2+} with Fe^{2+}, there is an additional advantage of facilitating heating by increasing the hysterersis-loop area under alternating magnetic fields, increasing the energy generation resulting from a single hysteresis loop. Even though the magnetic moments of samples are enhanced by substitution of Fe^{2+} with Co^{2+}, increase of coercivity from the Co^{2+} substitution could be hinderance of the magnetization reaction response time to AC magnetic field. Higher coercivity come with slower magnetization under alternating magnetic fields. By synthesizing nano-scale samples, one can get a super paramagnetic materials, suitable for self-heating hyperthermia application [11, 12]. In this study, nanoparticle samples of $Co_xFe_{3-x}O_4$ (x=0.2, 0.4, 0.6, 0.8, 1.0) were prepared, wherein Fe ions were replaced with Co ions on Fe_3O_4. Crystallographic studies using X-ray analysis, magnetization characteristics using VSM magnetization measurement, and heat effects under AC magnetic field using heat measuring device have been performed.

2. Experiments

Co-replaced $Co_xFe_{3-x}O_4$ (x=0.2, 0.4, 0.6, 0.8, 1.0) samples were prepared by high-temperature thermal decomposition (HTTD) method. The stoichiometric portion of Co and Fe raw materials, oleylamine, oleic acid, and

*Corresponding author: Tel: +82-2-910-4352
e-mail: sjkimmmm@kookmin.ac.kr

benzyl were heated to 200 °C for about 30 min. Further heating up to 300 °C for 1-hour was followed, then left to natural cool down to room temperature. The hexane and ethanol were mixed and separated 3 times using a centrifuge reactor for pure composition of $Co_xFe_{3-x}O_4$.

After almost 24-hour drying under a vacuum, final nanoparticles were obtained.

The crystallinity was investigated using X-ray diffraction with Cu-K_α (λ=1.5406 Å) radiation. The structural determination of $Co_xFe_{3-x}O_4$ (x=0.2, 0.4, 0.6, 0.8, 1.0) was performed by using the FullProf Suite program along with the Rietveld refinement method.

The magnetic properties were investigated by using a vibrating sample magnetometer (VSM). The magnetic hysteresis was measured by applying a magnetic field in the range of ±15 kOe. Experiments on the self-heating measurement of manufactured nanoparticles were conducted using MagneTherm equipment, which was optimized for measuring thermal effect of nanoparticles. The measurement was carried out under a frequency of 112 kHz, and 250 Oe applied magnetic field.

3. Results and Discussion

Fig. 1 shows XRD spectra for the $Co_xFe_{3-x}O_4$ (x=0.2, 0.4, 0.6, 0.8, 1.0).

The analysis shows the cubic structure with a space group of Fd-3m. No secondary structural phase is formed in synthesized samples and demonstrates a single structural phase clearly. Based on the Rietveld refinement, the Bragg-factor (R_B) and the F-factor (R_F) are listed in Table 1.

The lattice constant has determined to be 8.3759 Å for the x=0.2 sample and increases up to 8.3965 Å for the x=1.0 with Co doping amount. The linear increase of lattice constants as the doping amount (x) is due to the increase of doped portion of Co^{2+} ion with larger radius than that of the Fe^{2+} ion. [13].

Fig. 2 shows the results of magnetization experiments with the application of a 15 kOe external magnetic field.

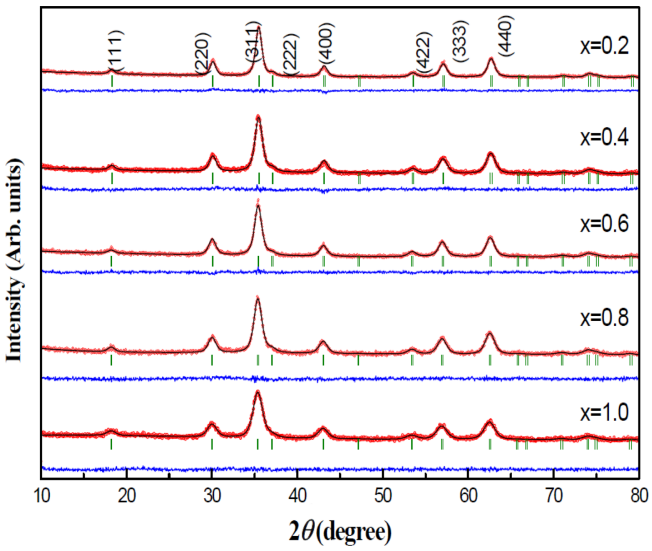

Fig. 1. (Color online) Rietveld refinement of XRD patterns of samples $Co_xFe_{3-x}O_4$ (x=0.2, 0.4, 0.6, 0.8, 1.0).

The samples exhibit soft-magnetic characteristics; rapid increase of magnetizations under the small external magnetic field (about a few hundred Oe) area, reaches saturation stage, and then a nearly flattens in the saturated region. To understand the hysteresis loop curves, we notice the magnetic ground state of typical Fe_3O_4 and $CoFe_2O_4$. In general, Fe_3O_4 bulk samples are known to have a soft-magnetic character with tens of Oe coercivity, while $CoFe_2O_4$ is known to be a hard-magnetic material with several kOe of coercivity [14].

In contrast, samples synthesized in this study show a behavior as if they have soft-magnetic characteristics as shown in Fig. 2. For this reason, we would like to point out that the samples produced in this study are nano-sized particles. To reckon the size of particles, Rietveld refinement method was carried out for the crystal analysis. The results are given in Table 1. In determining the particle size of the crystal, the line width of the main peak of the diffraction line was determined by using Debye-Scherr Equation.

Table 1. Results for X-ray refinement parameters of $Co_xFe_{3-x}O_4$ (x=0.2, 0.4, 0.6, 0.8, 1.0).

x	a_0	2θ (deg.)	D (Å)	Vol (Å^3)	β (deg.)	R_B(%)	R_F(%)
0.0	8.3758	35.520	20.5	587.6	0.8405	5.85	4.11
0.2	8.3759	35.518	20.2	587.4	0.8476	4.71	3.6
0.4	8.3819	35.491	17.2	588.9	1.0254	6.96	5.04
0.6	8.3840	35.481	17.9	589.3	0.9941	2.36	1.68
0.8	8.3889	35.461	16.4	590.4	1.1128	5.85	4.76
1.0	8.3965	35.418	16.8	592.0	1.1331	1.54	1.17

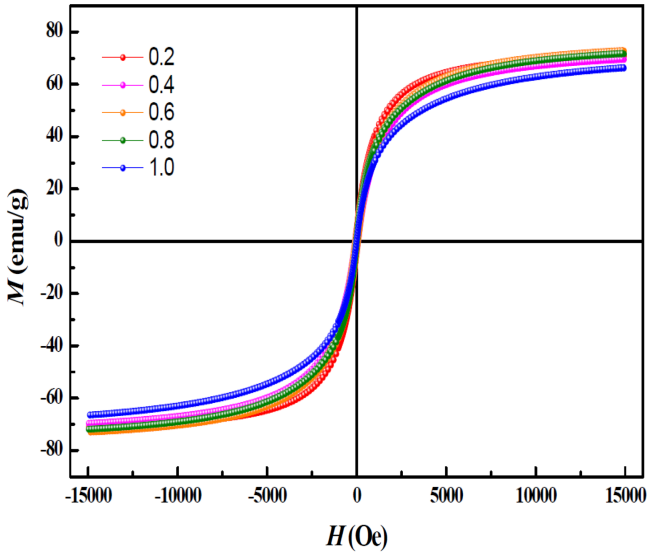

Fig. 2. (Color online) Magnetic hysteresis loops for the samples $Co_xFe_{3-x}O_4$ (x=0.2, 0.4, 0.6, 0.8, 1.0).

$$D = \frac{0.9\lambda}{\beta\cos\theta} \quad (1)$$

Here, D is the diameter of particle size, λ is wavelength of Cu-K_α (λ=1.5406 Å), β is FWHM (full width at half maximum), and θ is pick position of Bragg diffraction. The particle sizes are determined to 20.2 nm for x=0.2 and 16.4 nm for x=0.8. The range of the particle sizes are about 16~20 nm. These values are much smaller than those of bulk size magnetic materials (typically about hundreds nm).

Fig. 3 shows the magnetic coercivity (*Hc*) and saturation magnetization (*Ms*) obtained from Fig. 2.

For x=0.2 sample, the values of M_s and H_c were 71.0 emu/g and 84.0 Oe, respectively. For x=0.8 sample, those values were *Ms*=71.8 emu/g and *Hc*=40.5 Oe respectively.

In Fig. 3, the saturation magnetization values of the all the Co doped samples are 60~70 emu/g, and the values of the coercivity for the corresponding samples are distributed in the range of 40~98 Oe. All the values of the coercivity force are less than 100 Oe. Those are compared to traditional bulk Co^{2+} doped samples. In Co^{2+} doped bulk materials, the large magnetic moment and higher coercivity originated from magnetic anisotropy are exhibited, that is due to strong L-S coupling of Co^{2+} or is to the large contribution of none zero orbit-angular momentum of Co^{2+} [15]. As shown in Fig. 2, one can see that it shows a ferromagnetic interaction between neighboring atoms, being manifesting a ferromagnetic behavior in the hysteresis-loop. Magnetic hysteresis loop behavior of Co^{2+} doped nanoparticles is, however, different from

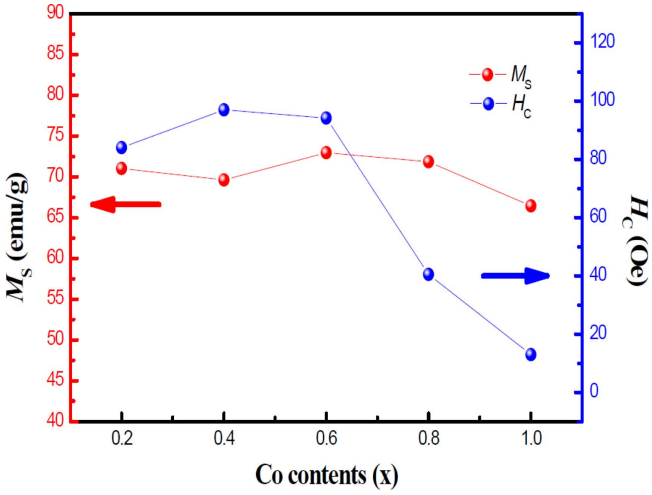

Fig. 3. (Color online) The values of saturation magnetization and coercivity for the samples $Co_xFe_{3-x}O_4$ (x=0.2, 0.4, 0.6, 0.8, 1.0) at room temperature.

the typical appearance of samples with large coercivity [16]. The size of the coercivity, however, shows a value pursuant to soft-magnetic form.

This is elucidated by the particle size of the crystal being small enough that the anisotropy interaction between the small boundaries of the region does not appear, thus displaying superparamagnetic properties of nanoparticles [17-19].

Fig. 4 shows the temperature dependence of the heating time of the $Co_xFe_{3-x}O_4$ (x=0.2, 0.4, 0.6, 0.8, 1.0) using the MagneTherm system. The conditions for the magnetic field and frequency used in the experiment were 250 Oe

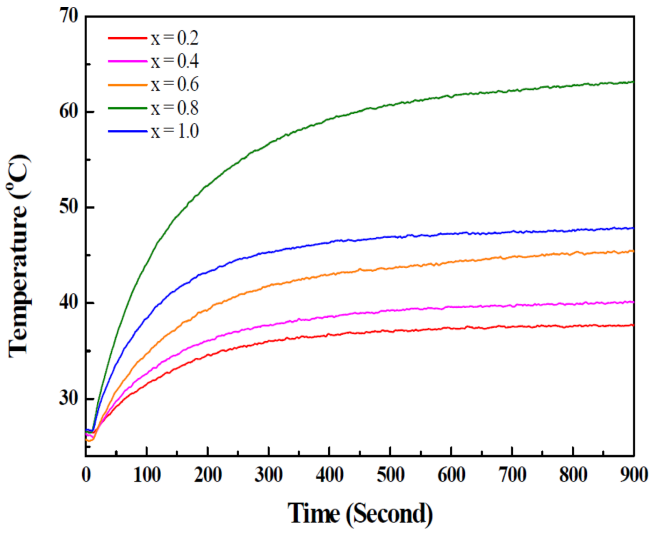

Fig. 4. (Color online) Self-heating temperatures of the nano particles $Co_xFe_{3-x}O_4$ (x=0.2, 0.4, 0.6, 0.8, 1.0) at 250 Oe, under a frequency of 112 kHz.

for the magnetic field and 112 kHz for alternating current frequency. The self-heating temperature ranged from 37.7 °C for the x=0.2 sample up to 63.2 °C for x=0.8 sample but after that; decreased to 47.8 °C for the x=1.0 sample. The results show that there is a critical boundary which affects the heating characteristic of Co replacement between the samples x=0.8 and x=1.0 [20].

4. Conclusion

In summary, we have manufactured $Co_xFe_{3-x}O_4$ (x=0.2, 0.4, 0.6, 0.8, 1.0) nanoparticle samples using high temperature thermal decomposition (HTTD) method. Each sample has a cubic structure with a group of Fd-3m space. The linear dependence on Co doping amount to lattice constant increase from 8.3759 Å for x=0.2, to 8.3965 Å for x=1.0. The fabricated particles sizes are about 16~20 nm. Low coercivity and rapid magnetization under small external magnetic field (a few hundred Oe) supports successful fabrication of superparamagnetic nanoparticles. Low magnetic field switch-on is suitable to achieve better hyper-thermionic. Doping Co is accompanied by trade-off of magnetic moment and coercivity but it is overcome by fabricating superparamagnetic nanoparticles.

Acknowledgement

This research was supported by Basic Science Research Program through the National Research Foundation of Korea (NRF) funded by the Ministry of Education (grant No. 2017R1D1A1B03).

References

[1] S. Kellenberger, A. Rosenthal, A. Myklatun, G. G. Westmeyer, G. Sergiadis, and V. Ntziachristos, Phys. Rev. Lett. **116**, 108103 (2016).
[2] D. Yoo, H. Jeong, S.-H. Noh, J.-H. Lee, and J. Cheon, Angew. Chem. Int. Ed. **52**, 13047 (2013).
[3] H. Huang, S. Delikanli, H. Zeng, D. M. Ferkey, and A. Pralle, Nat. Nanotechnol. **5**, 602 (2010).
[4] L. C. Branquinho, M. S. Carrião, A. S. Costa, N. Zufelato, M. H. Sousa, R. Miotto, R. Ivkov, and A. F. Bakuzis, Scientific Reports **3**, 2887 (2013).
[5] I. Sato, M. Umemura, K. Mitsudo, H. Fukumura, J.-H. Kim, Y. Hoshino, H. Nakashima, M. Kioi, R. Nakakaji, M. Sato, T. Fujita, U. Yokoyama, S. Okumura, H. Oshiro, H. Eguchi, I. Tohnai, and Y. Ishikawa, Sci. Rep. **6**, 24629 (2016).
[6] S. J. Kim, H. Choi, J. T. Lim, and C. S. Kim, J. Korean Phys. Soc. **68**, 403 (2016).
[7] J. Park, H. Choi, S. K. Kim, and C. S. Kim, AIP Adv. **8**, 056113 (2018).
[8] M. Jeun, S. Park, G. H. Jang, and K. H. Lee, ACS Appl. Mater. Interfaces **6**, 16487 (2014).
[9] J. H. Park, J. Son, H. Kim, S. Lee, S. J. Kim, and C. S. Kim, J. Korean Phys. Soc. **7**, 112 (2018).
[10] H. Choi, S. J. Kim, E. H. Choi, and C. S. Kim, IEEE Trans. Magn. **51**, 2003604 (2015).
[11] R. Sagayaraj, S. Aravazhi, C. S. Kumar, S. S. Kumar, and G. Chandrasekaran, SN Appl. Sci. **1**, 271 (2019).
[12] S. Nasrin, F. U. Z. Chowdhury, and S. M. Hoque, J. Magn. Magn. Mater. **479**, 126 (2019).
[13] M. S. Angotzi, V. Mameli, A. Musinu, and D. Nižňanský, J. Nanosci. Nanotech. **19**, 5008 (2019).
[14] M. Estrader, A. L-Ortega, S. Estradé, I. V. Golosovsky, G. S-Alvarez, M. Vasilakaki, K. N. Trohidou, M. Varela, D. C. Stanley, M. Sinko, M. J. Pechan, D. J. Keavney, F. Peiró, S. Suriñach, M. D. Baró, and J. Nogués, Nat. Commun. **4**, 2960 (2013).
[15] S. R. Naik, A. V. Saik, S. M. Yusuf, and S. S. Meena, J. Alloys Compd. **54**, 566 (2013).
[16] J. F. Hochepied and M. P. Pileni, J. Appl. Phys. **87**, 2472 (2000).
[17] X. Zhang, Y. Liu, and G. Qin, Appl. Phys. Lett. **106**, 033105 (2015).
[18] M. E. Sadat, R. Patel, S. L. Bud'ko, R. C. Ewing, J. Zhang, H. Xu, D. B. Mast, and D. Shi, Mater. Lett. **129**, 57 (2014).
[19] S. N. Kane and M. Satalkar, J. Mater. Sci. **52**, 3467 (2017).
[20] K. H. Chen, B. C. Chen, and C. Y. Ho, J. Nanosci. Nanotech. **18**, 3018 (2018).